

# Digital Printing of Optical Components

Donald J. Hayes, Ting Chen and David Wallace, MicroFab Technologies Inc. 1104 Summit Ave., #110, Plano, Texas USA

## Abstract

The use of direct write micro-printing for opto-electronic packaging is being accepted as a key enabling technology, specifically printing microlenses for optical interconnects and solders for electrical interconnects. This paper presents these two areas where micro-printing technology benefits opto-electronic packaging. For increasing light coupling efficiency, a microlens array is actively aligned and attached to a VCSEL array and photodiode array in smart pixel technology. A microlens array is also directly integrated with a VCSEL array in a wafer level fabrication. Solder jet is used for either bumping the VCSEL die or for directly connecting the VCSEL die with circuits on a substrate. By using micro-printing, components can have less part-count and smaller package size. The labor required for conventional optical alignment can be greatly reduced. Thus this technical advancement offers also cost effectiveness in manufacturing.

## Introduction

A piezoelectric micro-printing device, operating at drop-on-demand (DOD) mode, can reproducibly dispense spheres of fluid with diameters of 15 -100  $\mu\text{m}$  (volumes of 2pl - 5nl) at rates up to 25,000 per second [1]. The deposition is non-contact and data-driven. In combination with precision stages, the drops can be delivered to designated positions accurately. This technology has been developed to dispense fluids like solder alloys, optical polymers, and other adhesives. The deposition of optical polymers can form microlenses, waveguides, or other optical elements for shaping or guiding lights from photonic devices. The deposition of solders or adhesives can be used for attachment or bonding of opto-electronic components at different levels. Owing to the small and precise amount of material delivered, and also to the highly flexible process, this direct write micro-printing technology is being accepted as a key enabling technology for opto-electronic packaging. In this paper, we present the concept, process, and results of the applications of this technology in printing microlenses for optical interconnects and printing solders for electrical interconnects or structural features.

The majority of examples in this paper are given in the area of packaging VCSEL arrays. These examples show the advantages of this technology in the integration of optical and electric performance, and in reducing package size and assembly cost.

## Background of Micro-Printing

In a piezoelectric dispensing device the voltage pulse is applied to a piezoelectric transducer. The deformation of the transducer is coupled to the fluid at ambient pressure in a cavity and generates acoustic waves that result in the ejection of drops from the device orifice. In DOD operation, a drop is only ejected from the orifice when a voltage pulse is applied to the transducer [1]. The dispensed drop size is approximately equal to the orifice diameter. Figure 1 shows 50 $\mu\text{m}$  ethylene glycol drops from a DOD inkjet device at 2 kHz. The general fluid property requirements for

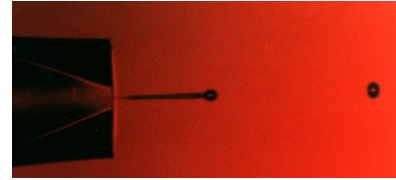


Figure 1. Dispensing of 50  $\mu\text{m}$  ethylene glycol drops at 2 kHz.

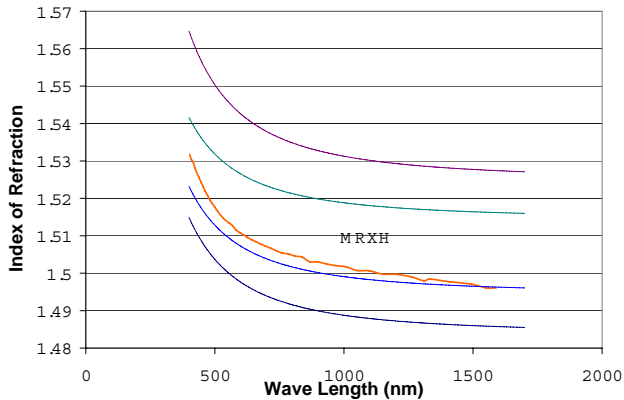
using a piezoelectric DOD dispensing device are: viscosity in the range of 0.5 - 40 cps and surface tension in the range of 20-70 dy/cm. Solder alloys need to be heated to molten states and need to have inert gas protection to prevent them from oxidization. Fluid samples with properties outside these ranges need to be heated or cooled to have the required rheological properties at the orifice of the device. In many applications the solidified optical polymer or solder is required to have certain profiles (such as hemispherical lens profile), or to have certain spreading areas. Therefore the substrate surface treatment can be important for the control of drop wetting and spreading. Shown in Figure 2 is a JetLab II dispensing platform developed and assembled at MicroFab for various printing tasks. This compact platform consists of sub-systems that include: print head, temperature and pressure control, X-Y-Z stages with motion control, machine vision system, spot UV delivery, and  $\text{N}_2$  co-flow.



Figure 2. A compact printing platform – JetLab II.

## Printing Micro-optics Using Polymer Jet

UV-curing optical epoxies are a preferred class of material for microlens printing, because of their thermal and chemical durability, as compared to other optical-grade polymers, such as acrylics, photoresists, and thermoplastics [2]. Our in-house developed MRXH-series of optical epoxy is a 100%-solid formulation of prepolymers. Its viscosity can be reduced to below 40 cps at temperatures above 100 $^{\circ}\text{C}$  to enable DOD printing. The dispersion curve of MRXH, along with that of other printable UV-curing acrylic polymers, is given in Figure 3. Printing the liquid prepolymer drops onto the designated locations, followed by UV



**Figure 3.** Dispersion curves of refractive indices of optical polymers, including optical epoxy MRXH.

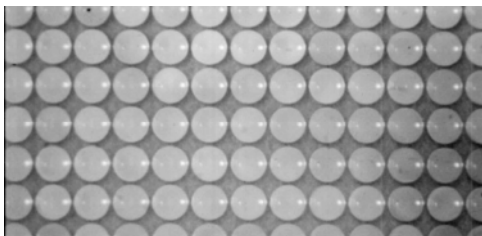


**Figure 4.** Printed microlens array of diameter  $916\mu\text{m}$  on  $1\text{ mm}$  centers with focal lengths of  $1.10\pm 0.01\text{ mm}$ .

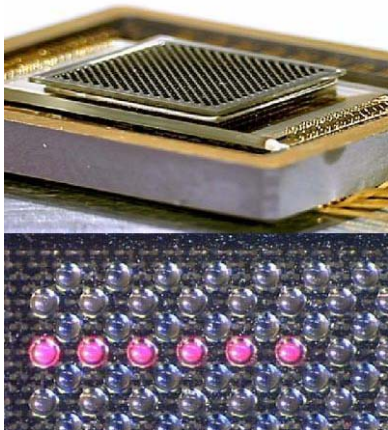


**Figure 5.** Smart pixel array module (top) and printed  $250\mu\text{m}$  diameter microlens array in module with VCSELs under. 6 VCSELs are turned on (bottom). (Photo courtesy of Honeywell)

and thermal curing cycles, forms hemispherical microlenses. The lens dimensions are determined by the number of the drops (i.e., the volume of dispensed material) and the condition of the substrate surface [3].

With micro-printing technology, microlens arrays have been fabricated with diameters ranging from  $50\mu\text{m}$  to  $5\text{mm}$  and lens speeds (F/#) from 1 to 4, shown in Figure 4 as an example. The highly uniform array has the diameter accuracy within  $\pm 1\mu\text{m}$  and the focal length accuracy within  $\pm 3\%$ . The printed and cured microlenses with MRXH-series material have passed a test at  $200^\circ\text{C}$  for 1 hour and have survived a 96-hour pressure pot test ( $120^\circ\text{C}$ , 100% RH). This thermal stability allows a solder re-flow

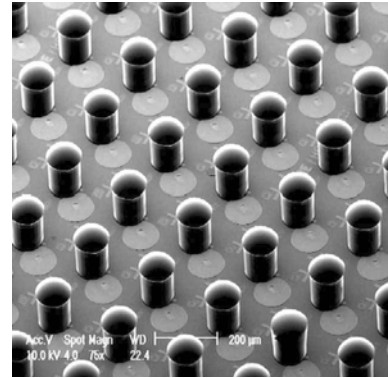


**Figure 6.** Pedestal-microlens structure fabricated on VCSEL wafer.

step in the modules assembly after the fabrication of microlenses [2,3].

Microlens arrays have been passively or actively aligned and attached with other components, such as VCSEL, laser diode, LED, and optical fiber, for efficient beam shaping and light coupling, since the light beams from all these photonic devices are highly diverging in nature. Figure 5 is an integration of microlens array in smart pixel array technology. The  $16\times 16$  microlens array ( $250\mu\text{m}$  diameter on  $500\mu\text{m}$  centers) is actively aligned with the VCSEL/ photodetector arrays that are integrated with Si ASICs [4].

We have also developed a wafer-level integration of micro-optics with VCSEL arrays [5]. Polymer pedestals are first formed on a VCSEL wafer through a photolithographic process of very-thick film patterning. Microlenses are then printed directly on top of the pedestals, as shown in Figure 6. The alignment of the pedestal to the VCSEL is defined by the photolithography tolerance, and the alignment of microlenses to pedestals is self-centering nature. The dimensions of pedestal and microlens are determined by means of optical modeling and by considerations of layouts of existing VCSEL wafer. The pedestals are  $115\mu\text{m}$  in diameter and  $100\mu\text{m}$  in height. The printed drop numbers are 3 to 7, corresponding to lens heights of 25, 28, 33, 36, and  $38\mu\text{m}$ . The improvement of optical performance is shown by the measured coupling efficiency from VCSELs to 50/125 multi-mode fibers. Figure 7 shows the coupling efficiency versus the axial distance between VCSEL emitting facet and fiber tip for different drop numbers in forming the microlenses. It is shown that the micro-optics with  $N = 6$  or 7 achieves the best performance.

This micro-optical structure has proved to high mechanical stability. It has sustained the follow-on wafer dicing and die bonding environment. This wafer-level integration reduces the part count, in comparison with individual VCSEL arrays, microlens arrays, spacers, etc.; eliminates the active alignment of microlens array to VCSEL array; reduces the total size of the component; and, thus lowers the total fabrication cost. Microlenses have also been printed on the tips of single mode or multi-mode optical fibers using glass collets to form monolithic linseed fibers for increasing efficiency of light coupling or collection [2,3].

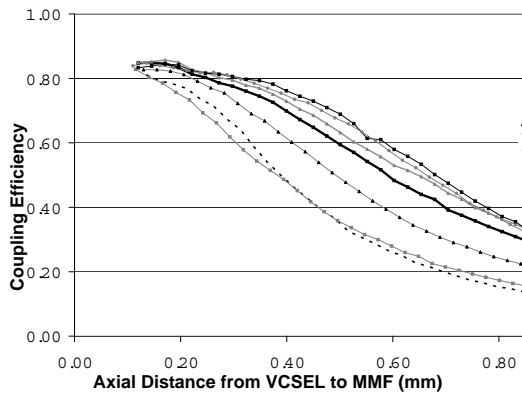


**Figure 7.** Coupling efficiency from VCSEL to MMF for different epoxy drop number  $N$  printed on pedestals to form microlenses. Parameters are given in the text.

## Electrical Interconnect Using Solder Jet

Deposition of small solder balls onto the interconnect pads of integrated circuits or chip-scale-packages is a large, rapidly growing application in electronic assembly, driven by flip-chip and other space/weight saving electronics packaging developments. Opto-electronic assembly processes that use surface tension driven self-centering to enable alignment of optical components to  $<1\mu\text{m}$  are also beginning to be used. Micro-printing technology provides one method to deposit solder bumps for these applications, and its use is being explored by many organizations. DOD mode solder jetting systems using both electro-dynamic and piezoelectric actuators have been developed [6]. Piezoelectric driven solder jetting developments are discussed below as examples of this application.

Operating characteristics for solder dispensing using piezoelectric DOD mode systems include: formation of spheres with diameters of  $25\text{-}125\mu\text{m}$ ; drop formation rates up to 1,000 per second; deposition onto pads at up to 600 per second; and operating temperatures up to  $320^\circ\text{C}$ . The solder dispensed has been primarily eutectic tin-lead ( $63\text{Sn}/37\text{Pb}$ ), but a number of other solders have been demonstrated, including high lead ( $95\text{Pb}/5\text{Sn}$ ), lead free ( $96.5\text{Sn}/3.5\text{Ag}$ ;  $97\text{Sn}/2.5\text{Ag}/0.5\text{Cu}$ ; indium;  $52\text{In}/48\text{Sn}$ ); and low temperature bismuth solders. Figure 8 shows the results of printing solder onto an  $18\times 18$  test coupon with  $100\mu\text{m}$  diameter pads on  $250\mu\text{m}$  centers. The deposited solder volume is equivalent to a drop with a diameter of  $100\mu\text{m}$ . Note that the bump shape shown in Figure 8 is a consequence of rapid ( $<100\mu\text{s}$ ) solidification. The instantaneous droplet rate for these tests was 400 per second and the pattern was printed by rastering the substrate in the horizontal direction of the figures. An average placement error of  $8\mu\text{m}$  was achieved in these tests, which is close

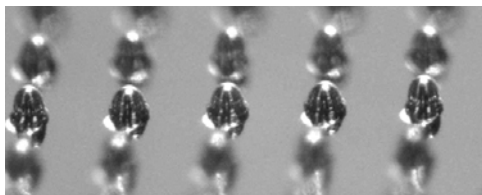


**Figure 8.**  $100\mu\text{m}$  diameter solder bumps placed onto  $100\mu\text{m}$  pads on  $250\mu\text{m}$  centers at 400 per second.

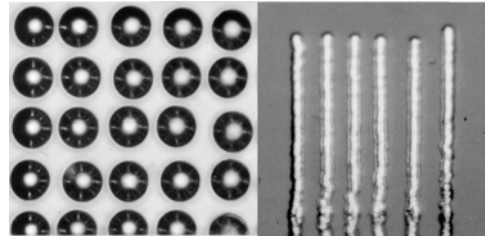


**Figure 9.**  $24\mu\text{m}$  diameter solder bumps on  $35\mu\text{m}$  centers (left), and an array of  $24\mu\text{m}$  towers (right).

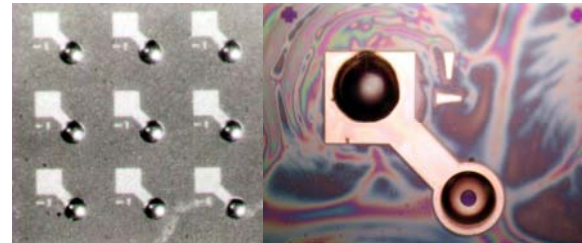


**Figure 10.** VCSEL array with printed  $90\mu\text{m}$  microlenses on emitters (left); VCSEL with microlens on emitter and  $60\mu\text{m}$  solder bump on bonding pad (right).

to the accuracy limitations imposed by the positioning and alignment systems of the platform employed. This method is continuous over the entire range of achievable volumes. Figure 9 shows an array of  $24\mu\text{m}$  diameter solder bumps on  $35\mu\text{m}$  centers, and an array of  $24\mu\text{m}$  towers formed by printing 100 drops of solder at the same X-Y position.

Solder and polymer have been printed on the same VCSEL array for bumping and forming microlenses. As shown in Figure 10,  $60\mu\text{m}$  diameter solder drops are deposited on the bonding pads, while the polymer drops are deposited on the emitter. Another example has a  $90^\circ$  configuration, in which the solder bumps directly interconnect the bonding pads on a  $1\times 4$  VCSEL array and the copper leads on the substrate. This direct bonding replaces the conventional wire bonding, which parasitic capacitance is one of the sources that limit the data transmission rate. To prevent the wide spreading of the solder after re-flow, Au-plated leads on the substrate are designed to have slot structure. The solder balls are printed to the slots and fill out the slots after re-flow to form stable junctions. As an example, the solder balls interconnect for the common cathode of the  $1\times 4$  VCSEL array with a Au-plated copper pad on the substrate is shown in Figure 11, before and after solder re-flow. Note that this VCSEL array already had integrated pedestals and microlenses on the anode side before solder bonding. The polymer components survived the solder re-flow at  $200^\circ\text{C}$ . The same  $90^\circ$  direct bonding has also been successfully applied to a photodiode array. Such highly compact optical and electrical interconnects will simplify the further integration of photonic devices with driving ICs and other chips. The compatibility of the solder bonding with the VCSEL performance is tested by comparing the DC characteristics of VCSELs and photodiodes before and after solder bonding. The results are given in Figure 12, in which the solid curves present the properties before solder bonding, while the cross marks present that after solder bonding. It is shown that the solder bonding has no significant impact to VCSEL's DC driving properties.

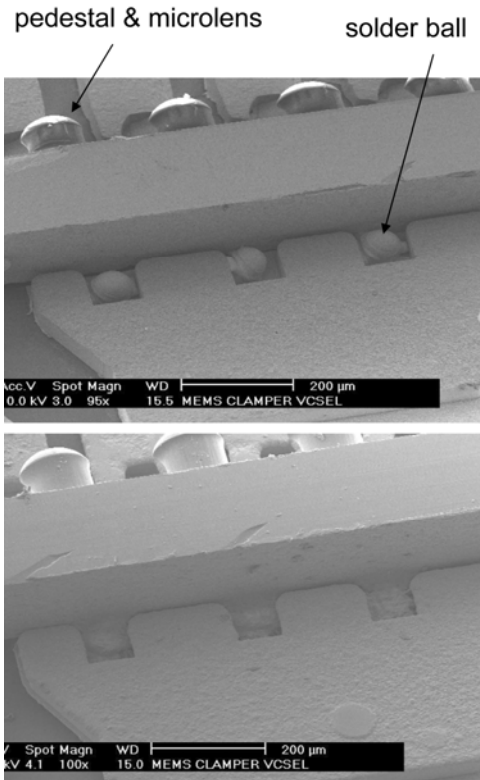


**Figure 11.** Solder balls interconnect cathode of VCSEL array die with Au-plated copper pad, before re-flow (top) and after re-flow (bottom).

## Conclusions

The capability of micro-printing technology to print optical polymers for microlenses and solder for solder interconnects have been demonstrated. This direct-write method provides opportunities for both significant cost reductions in existing components and for new component and device configurations.

## References

- [1] D.B. Wallace, W.R. Cox, and D.J. Hayes, "Direct Write Using Ink-jet Techniques," in "Direct-write Technologies for Rapid Prototyping Applications – Sensors, Electronics, and Integrated Power Sources", Alberto Pique and Douglas B. Chrisey, eds., pp. 177-227, Academic Press, San Diego, 2002.
- [2] W.R. Cox, C. Guan, and D.J. Hayes, "Microjet Printing of Micro-optical Interconnects and Sensors", in Optoelectronic Interconnects VII; Photonics Packaging and Integration II, Feldman et. al., eds, Proceedings of SPIE, Vol. 3952, pp. 400-407, 2000.
- [3] T. Chen, W.R. Cox, D. Lenhard, and D.J. Hayes, "Microjet Printing of High Precision Microlens Array for Packaging of Fiber-optic Components", in Optoelectronic Interconnects, Integrated Circuits, and Packaging, Eldada, Heyler, and Rowlette, eds., Proc. SPIE, Vol. 4652, pp. 136-141, 2002.
- [4] Yue Liu, "Heterogeneous Integration of OE Arrays with Si Electronics and Microoptics", IEEE Transactions on Advanced Packaging, Vol. 25, pp. 43-40, 2002.
- [5] T. Chen, D.J. Hayes, D.B. Wallace, A-K.C. Nallani, and J-B. Lee, "Inkjet Printing for Optical/Electrical Interfacing of VCSEL and PD Arrays", IMAPS International Symposium on Microelectronics Proceedings, pp. 864-868, 2003.

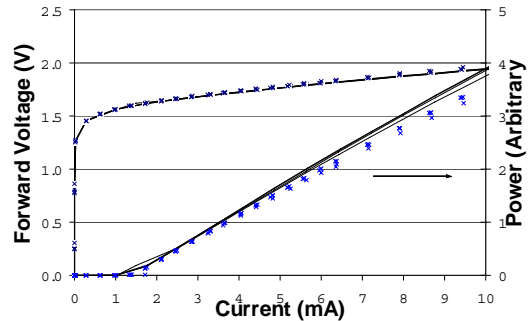


**Figure 12.** DC characteristics of VCSELs: solid curves – before solder bonding; cross marks – after solder bonding.

- [6] D.J. Hayes, W.R. Cox, and M.E. Grove, "Micro-jet Printing of Polymers and Solder for Electronics Manufacturing," Jour. Electronics Manufacturing, Vol. 8, pp. 209-216, 1998.

## Author Biography

*Donald J. Hayes is President of MicroFab Technologies, Inc. He holds a B.S. and M.S. in Physics from Louisiana State University and a Ph.D. in Materials Science from Rice. Under his leadership during the last 23 years, MicroFab has been a pioneer in the innovative use of ink-jet technology in electronics manufacturing, medical diagnostics, aroma generation, and many other applications. Dr. Hayes has been awarded 54 patents.*